

Large Lung Specimen Imaging Full-Field Micro-CT Using a High-Megapixel Single Lens Reflex Camera and Synchrotron Radiation

Keiji Umetani

Research & Utilization Division
Japan Synchrotron Radiation Research Institute
Hyogo, Japan
umetani@spring8.or.jp

Harumi Itoh

Faculty of Medical Science
The University of Fukui
Fukui, Japan
hitoh@u-fukui.ac.jp

Yoshiki Kawata, Noboru Niki

Department of Science and Technology
The University of Tokushima
Tokushima, Japan
kawata@tokushima-u.ac.jp,
c000028099@tokushima-u.ac.jp

Abstract—We have been developing large-field and high-resolution x-ray micro-CT systems using a 36M-pixel digital single lens reflex camera. The systems are highly specialized for large human lung specimen imaging of centimeter-sized objects with micrometer-range spatial resolution. The x-ray detector systems consist of a fluorescent screen for converting x-rays to a visible image, a pair of two interchangeable lenses, and the camera. The optical magnification in the lens system is determined using a ratio of two lens focal lengths. The lens coupling efficiency from the fluorescent screen to the camera through the lenses is important for high sensitivity. It is also determined by the two lenses. By changing the lens combination, widely various magnifications and sensitivities are readily obtainable. After the development of prototype systems for determining an optimum structure of an x-ray detector, a new practical system will be developed for higher sensitivity and higher resolution imaging.

Keywords—x-ray micro-CT; lung specimen; digital single lens reflex camera; high megapixel; synchrotron radiation

I. INTRODUCTION

Three-dimensional (3-D) microstructural analysis of human lung specimens with isotropic spatial resolution in the range of several micrometers has become increasingly important for the diagnosis of lung abnormalities during clinical routines of CT examinations [1–3]. Micro-CT scanners using synchrotron radiation play a crucially important role in imaging of lung micro-architectures. Nevertheless, the standard micro-CT setup does not satisfy field of view and spatial resolution requirements for large human lung specimen imaging.

To ascertain an optimum structure of an x-ray detector, first and second prototype micro-CT systems were developed in a cost-effective way using a 36M-pixel consumer-grade CMOS digital camera [4, 5]. The camera (D800e; Nikon Corp., Tokyo, Japan) is fitted with an image sensor with a 35.9 mm wide \times 24.0 mm high active area. The CMOS sensor has 7360 \times 4912 pixels, each of which is 4.88 μm \times 4.88 μm . Both prototype micro-CT systems use an identical 10- μm -thick phosphor screen for conversion from x-rays to a visible image.

The spatial resolution depends strongly on the phosphor screen thickness. Subsequently, for practical use, a new type of micro-CT system is under development using a new phosphor screen of around 6 μm thickness to achieve detector resolution of about 5 μm , which is comparable to the CMOS sensor pixel size of 4.88 μm .

II. METHODS

A. X-ray detectors

Cross-sections of the optical components of the x-ray detectors in Fig. 1 show how light passes through the optical assembly. Detectors used for the first and the second prototype micro-CT systems presented in Fig. 1(A) include a fluorescent screen, an optical mirror, a lens pair, and the 36-megapixel CMOS camera. X-rays are converted into a visible image in the approx. 10- μm -thick phosphor screen. The mirror behind the first lens deflects the luminescent light 90 deg upward to the second lens, which then focuses it on the camera.

The fluorescent screen unit includes an aluminum window for x-ray incidence and a 10- μm thick phosphor layer deposited on an optical glass. It is formed in a cladding-integrated structure. The cladding structure constrains the prototype detector design because the fluorescent screen unit is a commercial product having a particular structure. The new detector for the practical micro-CT system presented in Fig. 1(B) consists of similar components to those of (A). However, the fluorescent screen unit in Fig. 1(B) is a custom-made product for design (B) that is compact but well equipped.

For use in preliminary experiments, the first prototype micro-CT system was developed using two identical lenses with 135 mm focal length and a 2.0 F -number. However, the second lens observes not only the inside of the aperture of the first lens but also the outside of the lens housing in Fig. 1(A). To make the field of view of the second lens smaller than the aperture of the first lens, the field of view of the second lens must be reduced using longer focal-length lenses. The field of view of the micro-CT improved in the second prototype system using the two 180 mm focal length lenses.

However, the lens coupling efficiency from the fluorescent screen to the camera through the lenses is crucially important for high-sensitivity x-ray imaging. The respective efficiencies of the first prototype system and the second system are 3.76% and 1.97% [5]. The efficiency of the second system is lower than that of the first system because lenses with 180 mm focal length and a 2.8 F -number are used. For this reason, the new system adopted design (B) using two lenses with 135 mm focal length and the 2.0 F -number. The second lens does not observe the outside of the first lens housing in Fig. 1(B).

In the tandem lens configuration, the optical system comprises a pair of single-lens reflex camera lenses arranged face-to-face. The phosphor screen is placed in the focal plane of the first lens, whereas the image sensor is placed in the focal plane of the second lens. The optical magnification in the tandem lens system is determined by the ratio of the second lens focal length to that of the first lens. The optical systems in Fig. 1(A) have a fixed focal-length ratio of one to one. The CMOS sensor pixel has dimensions of $4.88 \mu\text{m} \times 4.88 \mu\text{m}$. An equivalent pixel size projected onto the fluorescent screen area is an identical value of $4.88 \mu\text{m}$ on a side because the magnification factor of the coupling lens system is 1.0. The x-ray field of view is $35.9 \text{ mm} \times 24.0 \text{ mm}$.

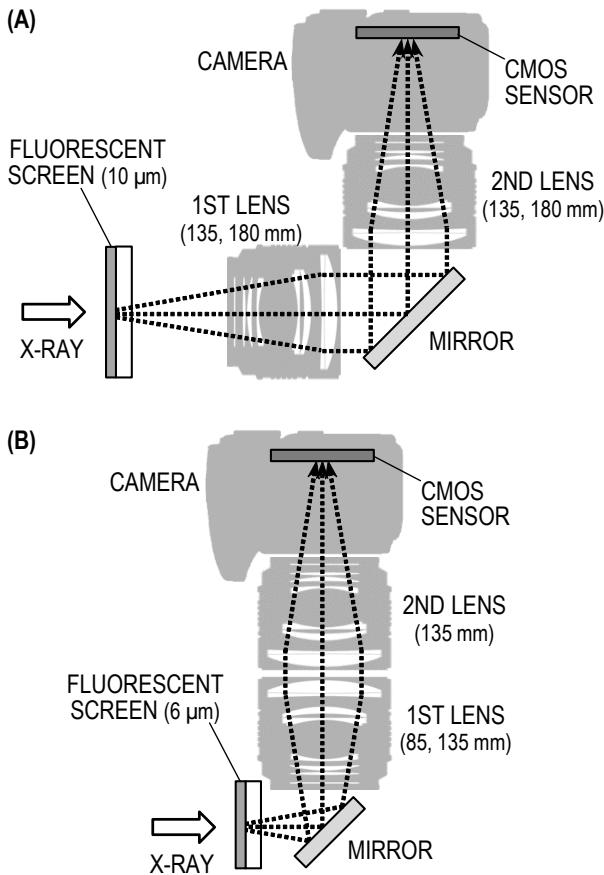


Fig. 1. Detector designs of two types: (A) the first and the second prototype micro-CT systems and (B) the new system for practical use.

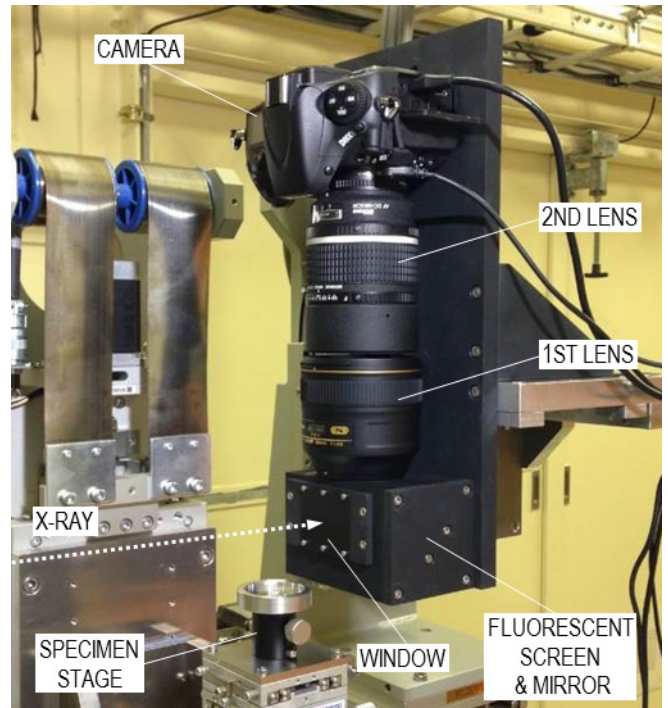


Fig. 2. Micro-CT system for large human lung specimen imaging using the new detector.

By changing the lens combination, widely various magnifications are readily obtainable for high-resolution imaging. Fig. 2 shows a micro-CT system for large human lung specimen imaging using the new detector. The optical system comprises the first lens with 85 mm focal length and the second lens with 135 mm focal length. In this case, an equivalent pixel size projected onto the fluorescent screen area is $3.07 \mu\text{m}$ on a side because the magnification factor of the coupling lens system is 1.59. The x-ray field of view also decreases to $22.6 \text{ mm} \times 15.1 \text{ mm}$. Moreover, the new system has a 6- μm thick fluorescent screen for higher spatial resolution imaging.

B. Synchrotron radiation micro CT

A useful source of synchrotron radiation is a storage ring, which uses bending magnets to maintain an electron beam at relativistic speeds in a closed trajectory. By bending the electron path, x-rays are emitted at each bending magnet in a direction that is tangential to the beam trajectory. A monochromator selects a single energy of synchrotron radiation. The monochromatic x-ray energy was thus adjusted by the monochromator to 15–25 keV to produce high-contrast images of lung specimens. The advantages of synchrotron radiation micro-CT compared with standard micro-CT are the following: The monochromatic x-ray beam prevents beam-hardening artifacts. The use of a nearly parallel beam enables exact CT reconstruction. Lung specimen imaging was performed at the SPring-8 BL20B2 beamline [5].

III. RESULTS AND DISCUSSION

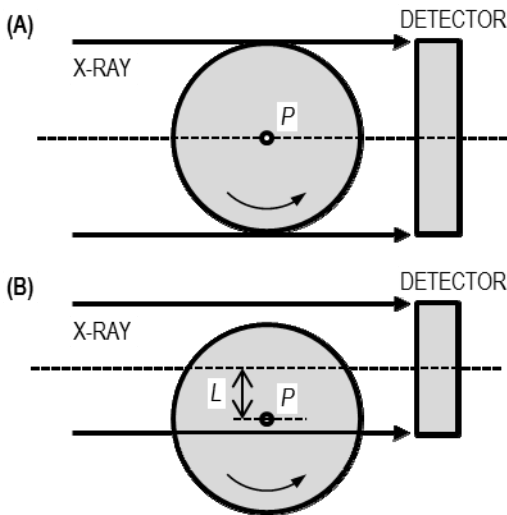


Fig. 3. Top views of two scan modes: (A) the specimen diameter fits within the detector's horizontal field of view and (B) the specimen diameter is larger than the field of view.

The lung specimen was set in an acrylic cylindrical case with 36 mm diameter and 40 mm height. The detector's x-ray fields of view are, respectively, 35.9 mm \times 24.0 mm and 22.6 mm \times 15.1 mm with the coupling-lens magnification factors of 1.0 (135 mm and 135 mm lenses) and 1.59 (85 mm and 135 mm lenses). In large-field imaging (35.9 mm \times 24.0 mm), the specimen fits within the detector's horizontal field of view as depicted in Fig. 3(A). Image signals are converted to digital data with a 7360 \times 4912-pixel, 14-bit format by an analog-to-digital converter in the camera. A personal computer system controls the camera for image acquisition. In all, 1800 projections were acquired over an angular range of 180 deg with angular step of 0.1 deg. Because the monochromatic x-ray beam is regarded as a parallel beam, the reconstruction was made with a filtered backward projection algorithm using the Shepp-Logan filter [6], providing data for a 7360 \times 7360 \times 4912 voxel image with an isotropic voxel size of 4.88 μ m.

In small field imaging (22.6 mm \times 15.1 mm), micro-CT imaging must be performed for the lung specimen beyond the scan field of view as depicted in Fig. 3(B). We used the offset scan mode, which meets the requirement that the imaging region of the scanned specimen must fit within a small field of view [7]. In Fig. 3(B), P is the center of the rotation stage; L is the offset distance away from the detector center. The offset scan mode involves 360 deg rotation of the rotational stage with angular step of 0.1 deg. The fundamental idea of the reconstruction from the offset scans is to reorganize the incomplete projections into the complete parallel-beam projections and to reconstruct CT images with the conventional filter back projection algorithm using the Shepp-Logan filter. The scan field of view using the offset scan mode is approximately twice as large as the field of view of 22.6 mm \times 15.1 mm. Then, we constructed a 13,220 \times 13,220 \times 4912 voxel image with an isotropic voxel size of 3.07 μ m.

Human lung specimens are inflated and fixed using Heitzman's method [8]. They are set as in vivo human lungs to the greatest extent possible, with preservation of the lung structure. In micro-CT imaging, the lung specimen was set in the acrylic cylindrical case with 36 mm diameter and 40 mm height. The acrylic case was placed on the specimen rotation stage in Fig. 2. Monochromatic x-ray energy was adjusted by the monochromator to 20 keV to produce high-contrast images of lung specimens. Fig. 2 shows that small field (22.6 mm \times 15.1 mm) micro-CT imaging was performed in the offset scan mode using a detector consisting of the first lens with the 85 mm focal length and the second lens with the 135 mm focal length. In all, 3600 projection images were acquired over an angular range of 360 deg with an angular step of 0.1 deg. The incomplete projections in the offset scan mode were reorganized into complete parallel-beam projections. CT images were reconstructed with the conventional back projection algorithm using the Shepp-Logan filter. Then, we obtained the 3-D isotropic volumetric data (13,220 \times 13,220 \times 4912 voxels) stacking the two-dimensional CT slice images with voxel resolution of 3.07 μ m \times 3.07 μ m \times 3.07 μ m.

After image reconstruction in CT, Fig. 4 presents a single tomographic slice of the lung specimen. Fig. 5 depicts an enlarged image of the area enclosed by the white rectangle in Fig. 4. The specimen in the cylindrical body of the acrylic case with 36-mm outer diameter is depicted by the large field of view imaging in Fig. 4. Yellow arrowheads in Fig. 5 indicate the secondary pulmonary lobule, which is the smallest fundamental unit in the lung and which is separated from neighboring secondary pulmonary lobules by the interlobular connective tissue septa indicated by the yellow arrowheads. The entire secondary pulmonary lobule is shown in the micro-CT image. Fig. 6 portrays an enlarged image of the area marked by the yellow dotted rectangle in Fig. 5. A dotted circle in Fig. 6 shows a single alveolus. In the numerous alveoli of the lung, gases are exchanged with surrounding capillaries of less than 10 μ m diameter. Each alveolus, with mean size of 200 μ m, is shown clearly in the image. Each is not round but polygonal, resembling a cell of a honeycomb.

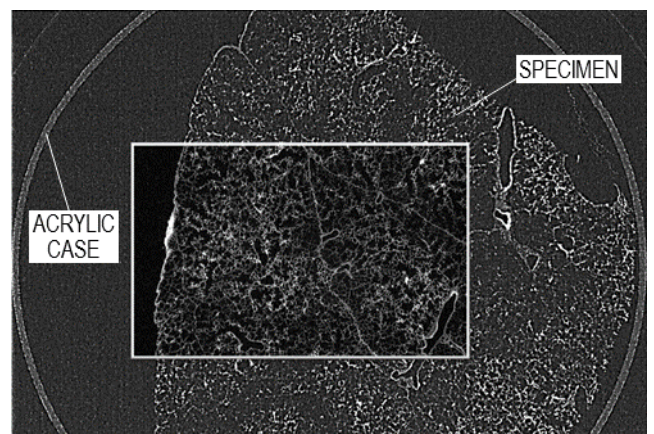


Fig. 4. Tomographic cross-section image of the human lung specimen.

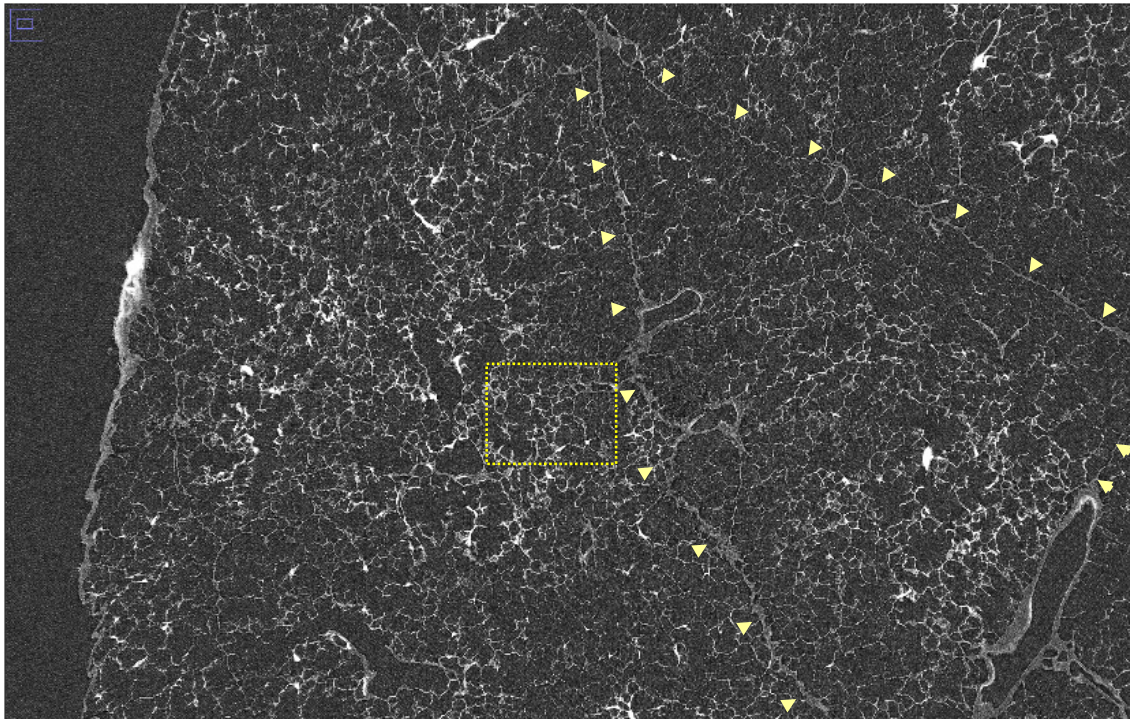


Fig. 5. Enlarged image of the portion marked by the white rectangle in Fig. 4. Yellow arrowheads indicate the secondary pulmonary lobule.

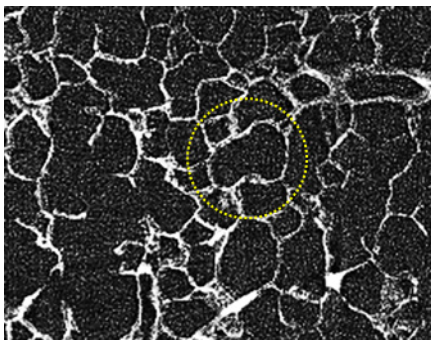


Fig. 6. Enlarged image of the area marked by the dotted rectangle in Fig. 5. A dotted circle shows a single alveolus.

IV. CONCLUSIONS

After development of prototype x-ray micro-CT systems using a 36M-pixel digital single lens reflex camera, a new practical system is under development for imaging having higher sensitivity and higher resolution. Using the new system, small-field ($22.6 \text{ mm} \times 15.1 \text{ mm}$) and high-resolution ($3.07 \mu\text{m}$) micro-CT imaging of the lung specimen was performed in the offset scan mode. 3-D images of the human lung specimen with columnar shape of about 36 mm diameter were obtained after reconstruction was made with a filtered backward projection algorithm. In a slice image, the whole specimen is depicted using large field of view imaging and micro-architectures of alveolar shape are visualized in the identical image. Successively, the development of a 50M-pixel micro-CT system has been undertaken to improve the spatial

resolution and field of view using a 50M-pixel digital single lens reflex camera.

This work was supported by JSPS KAKENHI Grant Number JP25240047. Experiments were performed at the BL20B2 and BL28B2 of SPring-8 with the approval of the Japan Synchrotron Radiation Research Institute (JASRI) (Proposal Nos. 2015A2062, 2015B1961, and 2016A1334).

REFERENCES

- [1] H. Itoh, M. Nishino, and H. Hatabu, "Architecture of the lung morphology and function," *J. Thorac. Imaging*, vol. 19, pp. 221-227, 2004.
- [2] W.R. Webb, "Thin-section CT of the secondary pulmonary lobule: anatomy and the image – The 2004 Feischner lecture," *Radiology*, vol. 239, pp. 322-338, 2006.
- [3] Y. Kawata, N. Kageyama, N. Niki, K. Umetani, K. Yada, H. Ohmatsu, N. Moriyama, and H. Itoh, "Microstructural analysis of secondary pulmonary lobule imaged by synchrotron micro CT using offset scan mode," *Proc. SPIE Medical Imaging*, vol. 7626, pp. 762610-1-9, 2010.
- [4] K. Umetani, Y. Kawata, N. Niki, and H. Itoh, "Development of 36M-pixel micro-CT using digital single-lens reflex camera," *Proc. 2015 IEEE Imaging Systems & Techniques (IST)*, 11-15, 2015.
- [5] K. Umetani, Y. Kawata, and N. Niki, "Development of 36M-pixel x-ray detector for large field of view and high-resolution micro-CT," *Proc. SPIE 10020, Photonics Asia, 10020005*, 2016.
- [6] A.C. Kak and M. Slaney, "Principles of computerized tomographic imaging," IEEE Press, 1988.
- [7] F. Jian, L. Hongnian, L. Bing, Z. Lei, and S. Jingjing, "X-CT imaging method for large objects using double offset scan mode," *Nucl. Instr. and Meth.*, vol. A575, pp. 519-526, 2007.
- [8] E.R. Heitzman, "The lung: radiologic-pathologic correlations," St. Louis, Mo, Mosby, 1984.